IOP Publishing Measurement Science and Technology
Meas. Sci. Technol. **35** (2024) 035115 (14pp) https://doi.org/10.1088/1361-6501/ad0f0e

Looking for optimal concentric ring electrodes: influence of design aspects on their performance

Javier Garcia-Casado[1,*], Yiyao Ye-Lin[1], Gema Prats-Boluda[1] and Oleksandr Makeyev[2]

[1] Centro de Investigación e Innovación en Bioingeniería, Universitat Politècnica de València, 46022 Valencia, Spain
[2] School of STEM, Diné College, Tsaile AZ 86556, United States of America

E-mail: jgarciac@ci2b.upv.es

Received 1 June 2023, revised 9 November 2023
Accepted for publication 22 November 2023
Published 14 December 2023

Abstract

Concentric ring electrodes (CREs) allow improved spatial resolution, reduced crosstalk and interference, and increased bandwidth in the sensing of bioelectrical activity. A wide variety of designs have been used, but their selection is rarely well-founded. The aim of this work is to assess the implications of aspects of CRE design such as the distance between poles, their width and their maximum diameter on aspects such as the signal amplitude (and, therefore, quality), Laplacian estimation error and spatial selectivity (SS). For this purpose, a finite dimensional model of the CRE was used, and its response to the activity of an electric dipole of variable depth was simulated via finite element method modeling. Our results show that increasing the electrode size increases the error to a greater extent than the signal amplitude increases. Pole widths should be as small as possible. The middle ring of the tripolar CRE should be as far away as possible from the central disc. Tripolar CREs typically outperform bipolar CREs of the same outer diameter, significantly reducing the Laplacian estimation error and improving the SS at the cost of a small decrease in signal amplitude. Our results also show that the design of current commercial versions of CREs can be optimized. Furthermore, we propose a methodology that facilitates the selection of an adequate CRE configuration based on the specifications for CRE performance and practical aspects, such as the depth of activity sources to be recorded from and/or the maximum size of electrodes to be used. The monitoring and analysis of bioelectrical signals in a wide range of applications can benefit from the enhanced electrode design and methodology proposed in this work.

Keywords: bioelectrical activity, concentric ring electrodes, Laplacian, optimization, finite element method modeling

Abbreviations:

BCRE	bipolar concentric ring electrode
CD	central disc
CRE	concentric ring electrode
*D*max	maximum diameter
IAD	inter-pole average distance
MR	middle ring
NA	normalized amplitude
NME	normalized maximum error
NSS	normalized spatial selectivity
OR	outer ring
SS	spatial selectivity
TCRE	tripolar concentric ring electrode
Z	dipole depth

* Author to whom any correspondence should be addressed.

1. Introduction

Concentric ring electrodes (CREs) are an alternative to conventional disc electrodes for the surface recording of bioelectrical signals. CREs are made up of a central disk (CD) and a series of outer concentric rings; those with one ring, i.e. the bipolar concentric ring electrode (BCRE) and with two rings, i.e. the tripolar concentric ring electrode (TCRE) are the most common versions.

CREs can directly estimate the Laplacian potential (the second spatial derivative of the surface potential) on the body surface in a simpler and more accurate way than discrete approximations derived from an array of disc electrodes measuring surface potentials [1]. A CRE acts as a filter that assigns more weight to the bioelectrical dipoles closer to the electrode, providing more detail in distinguishing multiple bioelectric dipole sources [2]. Therefore, one of the main benefits of CREs over disc electrodes is the enhanced spatial resolution, which has led to a better contrast to study the cardiac P-wave and its subcomponents than the traditional 12-lead electrocardiogram [3], more accurate identification of atrial fibrillation [4] and of cardiac depolarization waves on the body surface [5], better localization of activity in electroencephalogram movement-related potentials [1] and visual evoked potentials [6], and high-frequency activity in epileptic patients [7]. This enhanced spatial resolution also helps in reducing crosstalk and interference, facilitating the analysis and characterization of the target signal in a wide range of applications such as respiratory [8], uterine [9], intestinal [10], gastric [11], forearm [12, 13], masticatory [14] and swallowing muscle [15] myoelectrical recordings. Furthermore, due to their spatial filtering function [16], CREs have been shown to reduce the low-pass filtering effect on body surface recordings, providing signals with a greater bandwidth than conventional disc electrodes and closer to that of the intramuscular recordings obtained with needle electrodes [15, 17]. This permits picking up components of higher frequencies with relevant information, such as in electroencephalograms [18], or better assessing muscle fatigue [17].

Many different designs of custom-made and some commercial versions of CREs have been used. Nonetheless, the selection of the dimensional parameters, such as the outer diameter, pole widths for the CD and concentric rings, and inter-pole distances are poorly justified or not justified at all in experimental studies. The main criterion, when described, was to use BCREs with an outer diameter similar to the distance from the electrode to the activity source, based on preliminary studies by Kaufer *et al* [19], or to use poles of similar conductive areas to balance the electrode impedance [20]. The dimensional aspects of the CRE can have a great influence on their performance in terms of the spatial selectivity (SS) or signal amplitude and quality, as shown in different studies; for example, BCREs and TCREs have been compared, proving the superiority of the latter in terms of enhancing the spatial resolution and reducing mutual information [1, 16, 21]. It is also known that larger electrodes reduce the SS and increase the signal amplitude [3, 22, 23]. Nonetheless, working with real-life signals makes it difficult to study multiple aspects of electrode design, and typically only two versions of CRE (bipolar vs. tripolar, or two electrode sizes) are compared. Analytical and simulation studies can overcome these limitations, but they have been traditionally performed using a negligible dimensional model of a CRE, where the widths of the concentric rings and the radius of the CD are assumed to be negligible [21, 24, 25]. A realistic finite dimensional model of a CRE, which includes the radius of the CD and the individual widths of concentric rings, has been recently developed and validated [26, 27].

In this work, we aim to study the influence of CRE design aspects, such as the number of concentric rings (bipolar vs. tripolar), the outer electrode diameter, pole widths and inter-pole distances, on their performance in terms of the signal amplitude (and associated quality), Laplacian estimation error and SS. We also propose a methodology that permits the best set of dimensional parameters of the CRE to be chosen for a given application, taking into consideration practical aspects, such as the depth of activity sources and/or the maximum size of electrodes, as well as prioritized performance features of the CRE.

2. Materials and methods

2.1. Finite dimensional model of the CRE

In this work we compare different configurations of bipolar and tripolar CREs. In contrast to the negligible dimensional model of a CRE, the finite dimensional model considers that the CD has an outer diameter and that different concentric rings have inner and outer diameters that determine different pole widths; see figure 1. In a similar way to the inter-pole distance in the negligible dimensional model of a CRE, the distance between the median lines of each of the concentric ring poles defines the inter-pole average distance (IAD). Figure 1 shows the main dimensional parameters of the finite dimensional model of a TCRE. These are:

- Outer diameter of CD: D(CD)
- Inner diameter of middle ring: D(MR-inner)
- Outer diameter of middle ring: D(MR-outer)
- Inner diameter of outer ring: D(OR-inner)
- Outer diameter of outer ring: D(OR-outer)
- IAD between CD and middle ring: IAD(CD-MR)
- IAD between CD and outer ring: IAD(CD-OR)

For BCRE, definitions would be equivalent but with only one ring (R)

Similar to previous works [28, 29], the dimensions of the CRE in the finite dimensional model vary in a discrete fashion. Specifically, the maximum outer diameter of the CRE (Dmax) is subdivided into nine evenly spaced intervals. This yields more precise models than when using six intervals, which were also used in previous works [28, 29], and is considered a good balance between the number of different CRE configurations that can be assessed (146 for TCRE, 84 for BCRE) and the complexity of the computation and analysis.

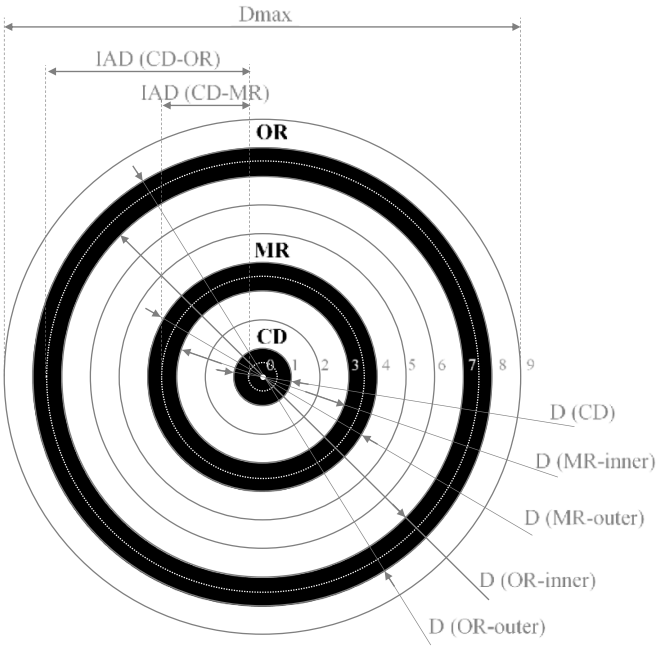

Figure 1. Finite dimensional model of tripolar concentric ring electrode [Trip1,4,8 →)−−)−−−)−]. CD: central disc; MR: middle ring; OR: outer ring; *D*max: maximum diameter; *D*: diameter; IAD: inter-pole average distance. The conductive area of each pole is shown in black. The median line of each pole is shown with a white dashed line. *D*max is subdivided into nine evenly spaced intervals.

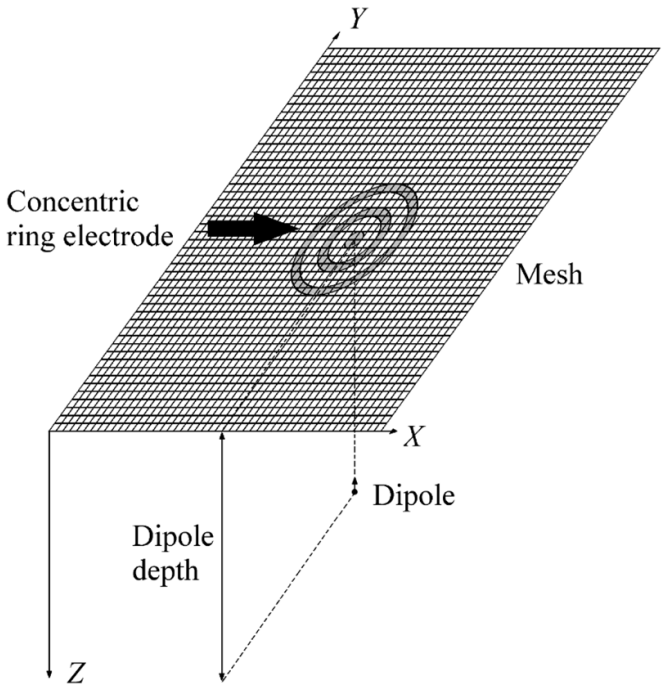

Figure 2. Schematic of the finite element method model used to compare the Laplacian estimates.

In this context, the following notation for a given configuration of a TCRE with *D*max will be used: 'Trip CD interval(s), MR interval(s), OR interval(s)'; e.g. Trip1,4,8 stands for a TCRE with a pole of CD corresponding to interval 1, an MR of interval 4 and an OR of interval 8 (shown in figure 1); Trip1-2,4-5,7-9 denotes a TCRE of a CD corresponding to intervals 1 and 2, an MR ranging from interval 4–5, and an OR ranging from interval 7–9. The notation of BCRE is equivalent but with only one ring, i.e. 'Bip CD interval(s), R interval(s)'; e.g. Bip1-3,9 denotes a bipolar CRE with a CD corresponding to intervals 1–3 and a ring of interval 9. A more visual complementary notation is also used, in which ')' represents intervals corresponding to poles and '-'represents intervals corresponding to blanks, e.g. Trip1,4,8 →)−−)−−−)−; Trip1-2,4-5,7-9 →))−))−))).

2.2. Finite element method model and calculation of electric and Laplacian potentials

The finite element method model from [1, 21, 24, 25, 30] was adapted from the negligible to finite dimensional model to directly compare the surface Laplacian estimates for different CRE configurations. Matlab (MathWorks, Natick, MA, USA) was used for all of the finite element method modeling. An evenly spaced 0.1389 mm square mesh of 1400 × 1400 points corresponding to roughly 20 cm × 20 cm was located in the first quadrant of the *X*–*Y* plane over a unit charge dipole oriented toward the positive direction of the *Z* axis and projected to the center of the mesh (see figure 2).

For a given dipole depth (Z), the electric potential v was generated at each point of the mesh [31]:

$$v = \frac{1}{4\pi\sigma}\frac{(\bar{r}_p - \bar{r})\cdot\bar{p}}{|\bar{r}_p - \bar{r}|^3} \tag{1}$$

where $\bar{r} = (x, y, z)$ is the location of the dipole, $\bar{p} = (p_x, p_y, p_z)$ is the moment of the dipole, and $\bar{r}_p = (x_p, y_p, z_p)$ is the observation point. The medium was assumed to be homogeneous with a conductivity σ equal to 7.14 mS cm^{-1} to emulate the biological tissue [32].

The analytical Laplacian Δv was calculated at each point of the mesh by taking the second spatial derivative of the electric potential v [31], as follows:

$$\Delta v = \frac{3}{4\pi\sigma} \times \left[5(z_p - z)^2\frac{(\bar{r}_p - \bar{r})\cdot\bar{p}}{|\bar{r}_p - \bar{r}|^7} - \frac{(\bar{r}_p - \bar{r})\cdot\bar{p} + 2(z_p - z)p_z}{|\bar{r}_p - \bar{r}|^5}\right]. \tag{2}$$

The following parameters were computed to characterize the electric and Laplacian potentials in the mesh:

Maximum signal amplitude (Max(v)): This is the greatest signal amplitude that can be recorded with a dipole at a given depth, i.e. the amplitude of a unipolar recording by means of

a disc electrode of negligible dimensions (punctual) located at the center of the mesh.

Maximum Laplacian amplitude (Max(Δv)): Maximum amplitude of the analytical Laplacian. It is obtained at the center of the mesh.

Spatial selectivity (SS): This assesses the decrease in the Laplacian amplitude from a given point to the surrounding neighbors at a certain displacement d in the X–Y plane [3, 5]. The greater the SS, the better the ability to differentiate the central signal from its neighboring signals. It is computed as the average of the ratio of the Laplacian potential from displacements at four cross-shaped points:

$$\mathrm{SS}\,(x_0, y_0, d) = \frac{1}{4}\left(\frac{\Delta v\,(x_0, y_0)}{\Delta v\,(x_0 - d, y_0)} + \frac{\Delta v\,(x_0, y_0)}{\Delta v\,(x_0 + d, y_0)} + \frac{\Delta v\,(x_0, y_0)}{\Delta v\,(x_0, y_0 - d)} + \frac{\Delta v\,(x_0, y_0)}{\Delta v\,(x_0, y_0 + d)}\right) \quad (3)$$

where (x_0, y_0) is the position where SS is calculated (the center of the square mesh) and d is the displacement.

2.3. Calculation of Laplacian estimates via CREs

In order to obtain the Laplacian estimates for different CRE configurations, bipolar differences for each of the ring potentials minus the CD potential (i.e. two for TCRE, one for BCRE) were linearly combined using the respective set of coefficients and divided by the square of the distance between the concentric circles [27]. The coefficients are obtained following the methodology described in [27]. For the example shown in figure 1 (Trip1,4,8), the coefficients are 111/337 and −146/3033 for bipolar signals MR-CD and OR-CD, respectively. Laplacian estimates were computed at each point of the mesh where the appropriate boundary conditions could be applied.

To obtain the bipolar signal(s) of each CRE configuration from the finite element method model, first, the potentials were calculated for the central point of the electrode, and for all nine concentric circles as the means of the potentials at four points on each circle. Next, this central point potential and these circle potentials were used to calculate the potentials on the recording surfaces (conductive area of electrode poles) of each CRE configuration. For example, the potential on the CD in the TCRE configuration in figure 1 (Trip1,4,8) is equal to the average of the potential at the center of the CD and the potential on the concentric circle with a diameter equal to one-ninth of Dmax; the potential of the MR is equal to the average of the potentials on concentric circles with diameters equal to 3/9 and four-ninths of Dmax, respectively. Then, the differences in electric potential between each ring and the CD of the electrode are computed.

2.4. Performance metrics of CREs

As stated in the previous section, Laplacian estimation via CREs is performed by linearly combining the bipolar signals resulting from the differential voltage of each ring and the CD [27]. The amplitude of such bipolar signals, and more specifically, the signal-to-noise ratio, can be of great importance to properly characterize the bioelectrical signal of interest [8, 15]. This amplitude obviously depends on the intensity, location and number of active electrical dipoles of the muscle or organ whose activity is being monitored and characterized. The power of noise and interference is also application-specific and depends on other factors, such as the crosstalk from other biological sources, skin-to-electrode impedance, instrumentation and acquisition devices. Nonetheless, a measure of the relative amplitude of bipolar signals from a CRE configuration with respect to the maximum amplitude that can be obtained in a given application is a valuable indicator of the potential robustness/quality of the signal and its derived parameters. Thus, the following CRE performance metric is defined:

Normalized (bipolar) signal amplitude (NA): This is the ratio between the bipolar signal amplitude(s) of the CRE (difference between the ring and CD potential) and the maximum signal amplitude. The greater the NA the better, in terms of the robustness of recorded signals to noise and interference. For a given dipole depth and CRE configuration, one value of NA is obtained for BCRE and two for TCRE. In the latter case, that of the MR will be smaller (and more restrictive) than that of the OR:

$$\mathrm{NA}^i = \frac{v\left(R^i\right) - v\left(\mathrm{CD}^i\right)}{\max\left(v\right)} \quad (4)$$

where i represents the CRE configuration, R^i is the ring for BCRE as well as the MR and OR for TCRE, and CD^i is the central disc of the CRE.

Other important aspects of the performance of a CRE configuration are related to its ability to correctly estimate the Laplacian potential and to provide a similar SS to the analytical one. We thus define the following measures (note that all metrics are normalized so that their values for different CRE configurations can be directly compared regardless of the dipole depth of a given application):

Normalized maximum error (NME): This is the NME of the Laplacian estimate of the CRE over the whole mesh surface. It is a common parameter to assess the accuracy of the Laplacian potential estimation [29]. The smaller the NME value, the more accurate the estimation:

$$\mathrm{NME}^i = \frac{\max\left|\Delta v - \Delta^i v\right|}{\max\left|\Delta v\right|} \quad (5)$$

Table 1. Dimensional parameters (expressed as a number of intervals) of CRE configurations used to study their influence on performance metrics. The dimensional parameter that changes with respect to a 'base' configuration is highlighted in bold. CRE: concentric ring electrode; CD: central disc; MR: middle ring; OR: outer ring; IAD: inter-pole average distance.

CRE		Width (CD)	Width (MR)	Width (OR)	IAD (CD-MR)	IAD (CD-OR)
Bip1,6 (base)	)----)---	1	—	1	—	5
Bip1,3	)-)------	1	—	1	—	**2**
Bip1,9	)-------)	1	—	1	—	**8**
Bip1-3,7	)))---)--	**3**	—	1	—	5
Bip1,5-7	)---)))--	1	—	**3**	—	5
Trip1,4,8 (base)	)--)---)-	1	1	1	3	7
Trip1,5,8	)---)--)-	1	1	1	**4**	7
Trip1,4,9	)--)----)	1	1	1	3	**8**
Trip1,3-5,8	)-)))--)-	1	**3**	1	3	7
Trip1,4,7-9	)--)--)))	1	1	**3**	3	7

where i represents the CRE configuration, $\Delta^i v$ represents the corresponding Laplacian estimate, and Δv represents the analytical Laplacian.

Normalized spatial selectivity (NSS): This is the ratio between the SS of the CRE and that of the analytical Laplacian at the center of the mesh. The displacement d is set to be equal to Dmax so that different CRE configurations can be directly compared:

$$\mathrm{NSS}^i = \frac{\mathrm{SS}^i}{\mathrm{SS}} \tag{6}$$

where i represents the CRE configuration, SS^i represents the SS of the CRE, and SS represents the SS of the analytical Laplacian.

2.5. Comparison of CREs

When using CREs for the monitoring and characterization of the activity of a bioelectrical signal source, two application-specific parameters influence the CRE performance. The first one is the dipole depth (Z) of the organ/muscle to be studied; e.g. a few millimeters for superficial muscles versus 2–4 cm for the heart. The second one is the maximum size of the electrode (Dmax). This maximum size can depend on factors such as anatomical constraints and the number of CREs when using arrays or grids of electrodes, e.g. those used for body surface potential mapping as in [3–5, 33]. It should be noted that the spatial distribution of the electric potential on the CRE generated by the dipole is the same for a given Dmax/Z ratio, i.e. it would be a dimensional scaling factor of the finite element method model. Furthermore, since the CRE performance metrics are normalized, different combinations of Z and Dmax provide the same results as long as Dmax/Z is constant; e.g. for $Z = 0.5$ cm, Dmax $= 1$ cm and for $Z = 1$ cm, Dmax $= 2$ cm. Thus, the results obtained for the performance metrics of different CRE configurations can be more easily analyzed, and subsequently particularized for a given application, if computed for different Dmax/Z ratios. Note that we have preferred to use Dmax rather than the OR diameter of CRE so that we can also directly study the effects of not using all the available 'room' on the electrode. The performance comparison is performed for CREs with a Dmax/Z ratio ranging from 0.1 to 5.

For each Dmax/Z ratio, we also study the effects of the dimensional parameters of BCREs and TCREs, such as the width and IAD of different poles, on the performance of the electrode. The configurations tested for the BCRE and TCRE are shown in table 1.

Addressing the influence of the dimensional parameters of CREs on the performance metrics, we propose candidates for the optimal configurations of BCREs and TCREs for each metric. These optimal candidates are also compared to previous approaches to CRE optimization as well as to commercial CREs. In [34] and [29], we proposed optimal versions of BCRE and TCRE, respectively, with one criterion of minimizing the Laplacian estimation error and with the constraint that the outer diameter of the CRE should be Dmax. The optimal candidates were Bip1,3-9 and Trip1,3,5-9. Regarding commercial CREs, on the one hand, Spes Medica (Genova, Italy) commercializes CODE401526 with the diameter of the CD equal to 10 mm, and the internal and external diameters of the OR equal to 20 mm and 30 mm, respectively. Such electrodes would be equivalent to Bip1-3,7-9 and Dmax $= 30$ mm in our finite dimensional model of a CRE. On the other hand, CREmedical (Kingston, RI, USA) commercializes TCREs with the following diameters: 2.8 mm CD, 5.2–6.4 mm MR inner–outer, 8.8–10 mm OR inner–outer. Such electrodes can be approximated by Trip1-3, 6,9 and Dmax $= 10$ mm in our finite dimensional model of a CRE.

3. Results

3.1. Analytical values

Figure 3 shows the analytical values of the maximum signal amplitude (Max(v)), maximum Laplacian amplitude (Max(Δv)) and SS derived from the finite element method model for different dipole depths (Z). The amplitudes significantly decay (note the vertical logarithmic scale) as the dipole depth increases, with a steeper response for Max(Δv). The SS shows that for a given displacement (Dmax), the smaller the dipole depth, the greater the SS. It is noteworthy that the peak

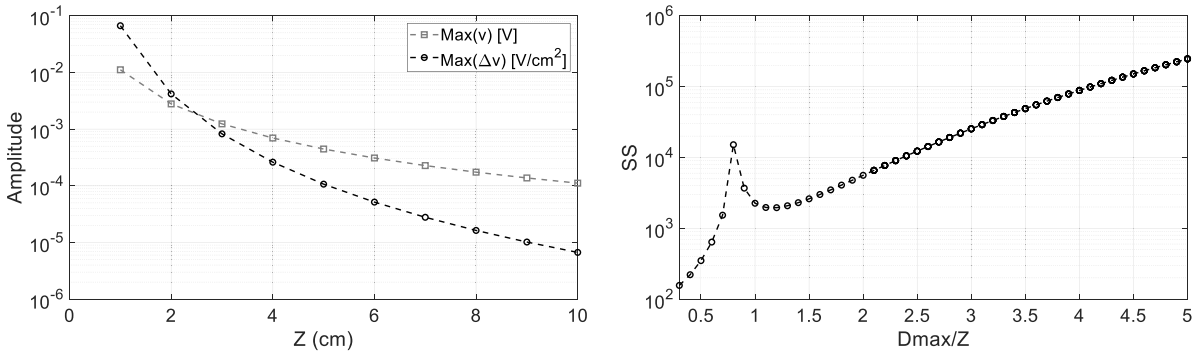

Figure 3. Left panel: Maximum signal amplitude (Max(v)) and maximum Laplacian amplitude (Max(Δv)) for different values of dipole depth (Z). Right panel: SS at the center of the mesh for different values of Dmax/Z (displacement d equal to Dmax).

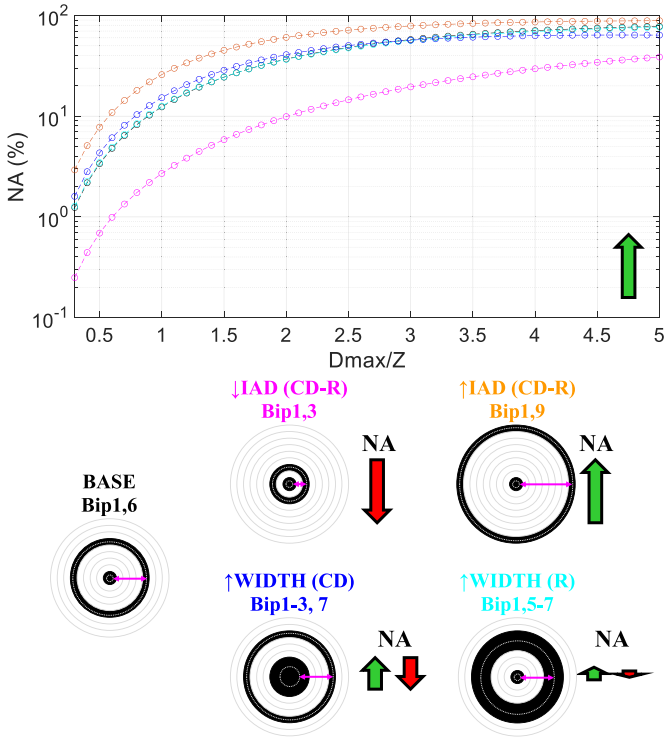

Figure 4. NA for different values of Dmax/Z and configurations of BCREs. The effect of changing Dmax/Z, IAD and pole widths on the NA is indicated with arrows of length corresponding to the strength of the effect, in green color if favorable and red if unfavorable. The NA of Bip1,6 almost overlaps with that of Bip1,5-7. Dmax: maximum diameter; Z: dipole depth; IAD: inter-pole average distance; CD: central disc; R: ring.

observed at points with a distance of about Dmax/$Z = 0.8$ from the center of the mesh is associated with a zero-crossing of the surface Laplacian amplitude, which is the denominator of the SS as shown in equation (3).

3.2. NA

Figure 4 shows the results of the NA depending on Dmax/Z for different configurations of BCRE. The effect of changing Dmax/Z, IAD and pole widths on the NA is indicated with arrows of length corresponding to the strength of the effect, in green color if favorable and red if unfavorable. The following text (and that of sections 3.3–3.5) systematically presents the results of the effects of these factors in separate paragraphs, with a final paragraph summarizing the potential optimal designs based on these effects.

It can be seen that the greater the Dmax/Z, the greater the NA for all BCRE configurations; i.e. for a given dipole depth and electrode configuration, the larger the electrode, the larger the NA. Electrode Bip1,6 is shown as a 'base' configuration: width = 1/9·Dmax for both poles and IAD (CD-R) = 5/9·Dmax.

To study the effects of increasing and reducing the IAD, the results of Bip1,9 and Bip1,3 are shown, where IAD (CD-R) increases to 8/9·Dmax and decreases to 2/9·Dmax, respectively, keeping the pole widths constant. When compared with the base BCRE configuration, it is observed that enlarging the IAD results in a considerable increase in the NA, and reducing the IAD considerably decreases the NA.

To study the effect of changing the width of CD and R, the results from Bip1-3,7 and Bip1,5-7 are shown, where the width is increased to 3/9·Dmax for CD and R, respectively, keeping the IAD (CD-R) and the width of the other pole constant. Comparison with the base electrode reveals that making CD wider results in a slight increase in NA for values of Dmax/$Z < 2.8$ and a slight decrease for greater values. Widening the ring of the electrode shows a similar trend for NA, but the changes are almost negligible.

It is also interesting to compare the NA of Bip1,9 for a given Dmax/Z with the NA of Bip1,3 for 3·Dmax/Z. Both configurations have the same 'true' outer diameter of the electrode but with the latter having absolute values of pole widths three times larger and IAD 3/4 smaller (the total equivalency of Bip1,3 (3·Dmax/Z) would be with Bip1-3,7-9 (Dmax/Z)). For example, NA[Bip1,9 (0.3)] = 2.9% vs. NA[Bip1,3 (0.9)] = 2.2% or NA[Bip1,9 (1)] = 25.9% vs. NA[Bip1,3 (3)] = 19.2%. These results show again that the influence of the IAD on the NA is greater than that of the pole width.

Considering the effects of the IAD and pole widths, candidates for the optimal configuration of BCRE in terms of maximizing the NA would be those with the largest IAD,

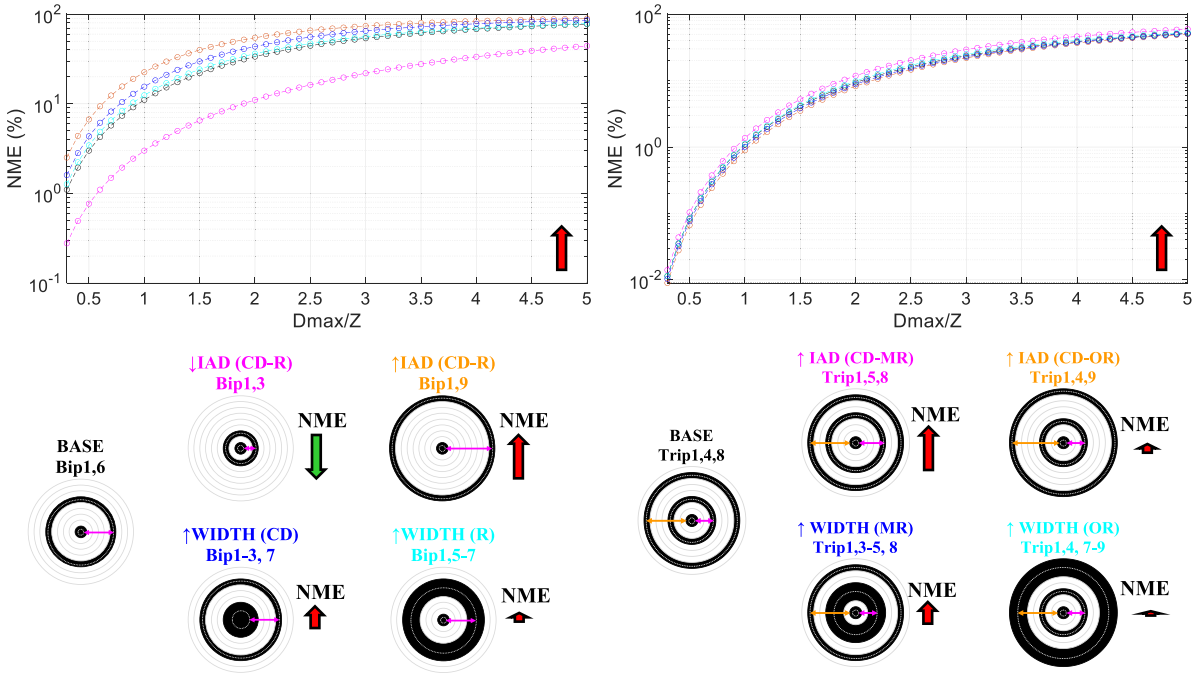

Figure 5. NME for different values of *D*max/*Z* and configurations of BCRE (left panel) and TCRE (right panel). The effect of changing the *D*max/*Z*, IAD and pole widths on the NME is indicated with arrows of length dependent on the intensity of the effect, in green color if favorable and red if unfavorable. *D*max: maximum diameter; *Z*: dipole depth; IAD: inter-pole average distance; CD: central disc; R: ring; MR: middle ring; OR: outer ring.

i.e. Bip1,9, and wider CD while keeping a large IAD, i.e. Bip1-3,9.

For tripolar CREs, two bipolar signals (MR-CD, and OR-CD) and two values of NA were obtained for each TCRE configuration and *D*max/*Z*. The results for each of these bipolar signals are not shown since they are equivalent to that of the analogous BCRE, deriving the same conclusions regarding the effects of the IAD and pole width. As IAD (CD-MR) is always smaller than IAD (CD-OR), the NA of bipolar signal from MR-CD is thus smaller (more restrictive). Candidates for the optimal configuration of TCRE in terms of maximizing the NA would thus be those with the largest IAD (CD-MR), i.e. Trip1,7,9, and wider CD while keeping a large IAD (CD-MR), i.e. Trip1-3,7,9.

For the same *D*max, the maximum NA that can be obtained from the MR of TCRE is smaller than from the ring of BCRE, and bipolar electrodes are thus better than tripolar in terms of this performance metric.

3.3. NME

Figure 5 shows the results of the NME depending on *D*max/*Z* for different configurations of BCRE (left panel) and TCRE (right panel). It can be observed that the NMEs of TCREs are significantly smaller than those of BCREs. The effect of changing the *D*max/*Z*, IAD and pole widths on the NA is indicated with arrows of length corresponding to the strength of the effect, in green color if favorable and red if unfavorable.

The NME increases for all CRE configurations as *D*max/*Z* does; i.e. for a given electrode configuration and dipole depth, the larger the electrodes, the greater the error. Electrodes Bip1,6 and Trip1,4,8 are shown as 'base' configurations for BCREs and TCREs, respectively, to study the influence of the IAD and pole width.

Figure 5 shows that increasing the IAD while keeping the pole widths constant results in unfavorable greater values of NME for bipolar and tripolar CREs. Similarly, increasing the width of poles while keeping the IAD constant yields greater values of NME for BCREs and TCREs. Increasing the width of the CD for TCRE is not shown for simplification, but also results in larger values of NME. It also seems that the influence of the IAD is greater than that of the pole width, and in the case of TCREs, those of the middle ring affect the NME to a greater extent than those of the outer ring.

The comparison of NME[Bip1,9 (0.3)] = 2.5% vs. NME[Bip1,3 (0.9)] = 2.4% or NME[Bip1,9 (1)] = 22.5% vs. NME[Bip1,3 (3)] = 21.9% shows that in this case the effects of greater absolute values of both pole widths and smaller IAD for Bip1,3 are virtually balanced out.

Considering the effects of the IAD and pole widths, candidates for the optimal configuration of BCREs and TCREs in terms of minimizing the NME would be those with the smallest IAD and smallest pole width, i.e. Bip1,3 and Trip1,3,5.

3.4. NSS

Figure 6 shows the results of the NSS depending on *D*max/*Z* for different configurations of the BCRE (left panel) and TCRE (right panel). It can be observed that, for a given value of *D*max/*Z*, the NSS of TCREs is greater than that of BCREs, indicating a better performance of TCREs in terms of the SS. The effect of changing the *D*max/*Z*, IAD and pole width on

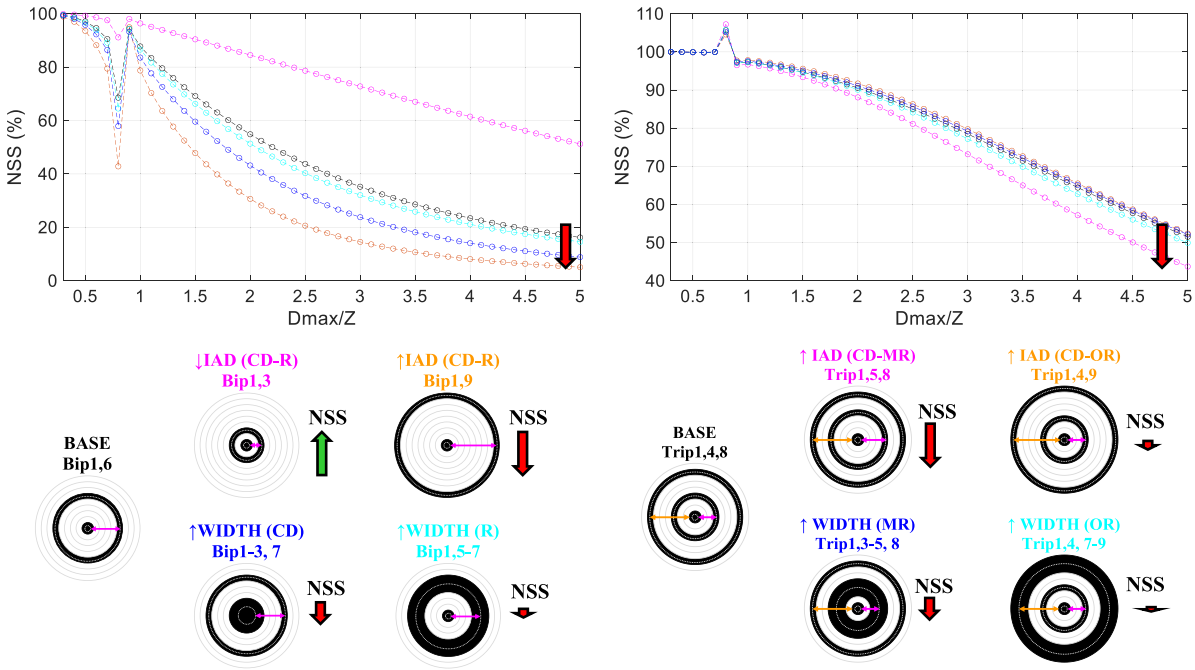

Figure 6. NSS for different values of *D*max/*Z* and configurations of BCRE (left panel) and TCRE (right panel). The effect of changing the *D*max/Z, IAD and pole widths on the NSS is indicated with arrows of length dependent on the intensity of the effect, in green color if favorable and red if unfavorable. *D*max: maximum diameter; *Z*: dipole depth; IAD: inter-pole average distance; CD: central disc; R: ring; MR: middle ring; OR: outer ring.

the NA is indicated with arrows of length corresponding to the strength of the effect, in green color if favorable and red if unfavorable.

It can be seen that the greater the *D*max/*Z*, the smaller the NSS for all CRE configurations, with the exception of the region surrounding *D*max/*Z* = 0.8, where the displacements result in an analytical Laplacian potential close to zero and the NSS cannot be directly interpreted since its value is highly dependent on the truncation error.

Figure 6 shows that increasing the IAD results in a decrease in the NSS for both BCREs and TCREs; i.e. in a worse performance of the CRE in terms of the SS. Such a decrease is less severe when enlarging the distance between the CD and OR, pointing to a greater importance of the IAD (CD-MR). Regarding the influence of the pole width, its effect is similar to that of the IAD, i.e. enlarging the pole width results in a smaller NSS of the CRE. In the case of TCREs, the influence of the width of the MR is greater than that of the OR, which is almost negligible, pointing again to a greater influence of the MR.

In general, the effects of the CRE dimensional parameters on the NSS are equivalent to those on the NME, and candidates for the optimal configuration of BCREs and TCREs in terms of maximizing the NSS would thus be those with the smallest IAD and smallest pole widths, i.e. Bip1,3 and Trip1,3,5.

3.5. NA/NME ratio

In sections 3.2 and 3.3, the effect of the dimensional parameters of CREs on the NA and the NME generally showed opposite behaviors, i.e. what increases the NA also increases the NME (and decreases the NSS; see section 3.4). Therefore, it is interesting to study which effect is more acute and which CRE configuration achieves the best balance between maximizing the amplitude (and therefore the associated signal-to-noise ratio) and minimizing the error in the Laplacian estimation. This can be assessed by computing the NA/NME ratio.

Figure 7 shows the results of this ratio for BCRE and TCRE when changing different aspects of the CRE design (e.g. IAD, width) in a similar way to figures 4–6. It is observed that TCREs remarkably outperform BCREs in balancing the NA and NME (note the linear scale for BCRE and logarithmic scale for TCRE). The effect of changing the *D*max/*Z*, IAD and pole widths on the NA is indicated with arrows of length corresponding to the strength of the effect, in green color if favorable and red if unfavorable.

As can be observed, the general trend is that the NA/NME diminishes as *D*max/*Z* increases (steeper for TCREs); i.e. the increase in the NME associated with the increase in the electrode size is greater than the increase in the NA.

Similarly, enlarging the widths of any pole of the BCRE and TCRE also results in a lower (worse) NA/NME ratio. This is observed when comparing CREs with the same IAD (blueish traces compared to black ones) and also with the same 'true' outer diameter as derived from the comparison of NA/NME of Bip1,9 (*D*max/*Z*) with Bip1,3 (3·*D*max/*Z*). Regarding the influence of the IAD, for BCRE it is favorable to enlarge it, for *D*max/*Z* < 2.5. In TCREs, when keeping the IAD constant (CD-OR), it is beneficial to increase the IAD (CD-MR), i.e. the NA increases to a greater extent than the NME.

Considering the effects of the IAD and pole width, candidates for the optimal configuration of BCREs in terms of

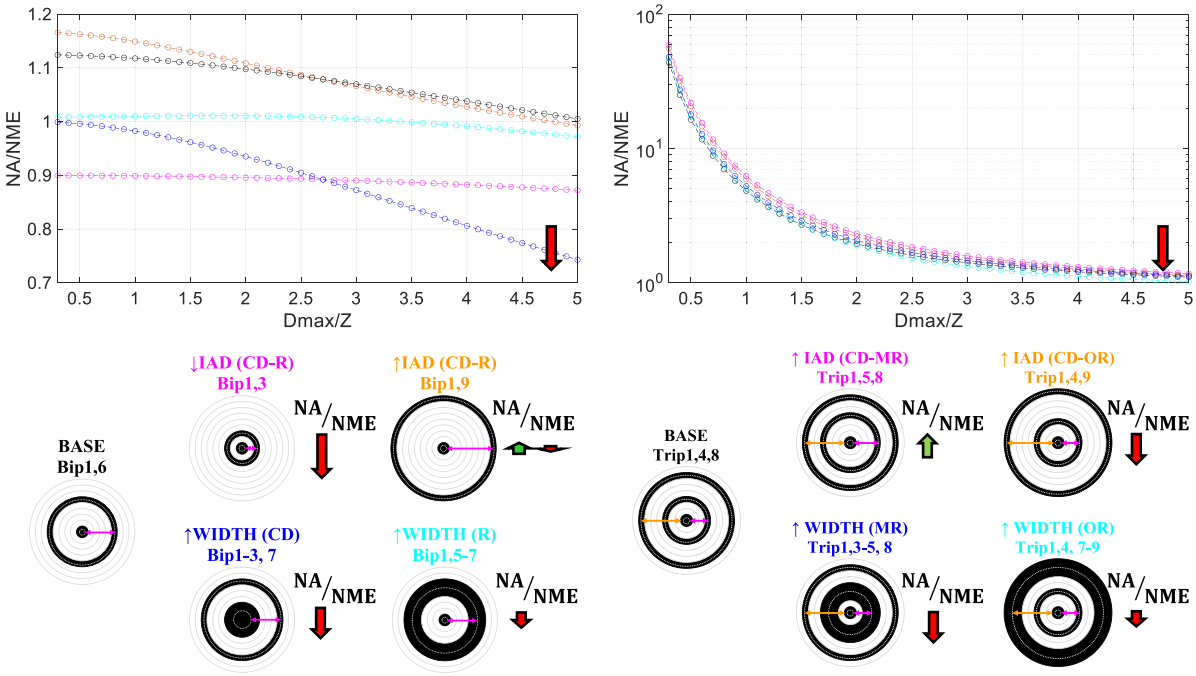

Figure 7. NA/NME ratio for different values of *D*max/*Z* and configurations of BCRE (left panel) and TCRE (right panel). The effect of changing *D*max/*Z*, IAD and pole widths on the NA/NME is indicated with arrows of length dependent on the intensity of the effect, in green color if favorable and red if unfavorable. NA: normalized amplitude; NME: normalized maximum error; *D*max: maximum diameter; *Z*: dipole depth; IAD: inter-pole average distance; CD: central disc; R: ring; MR: middle ring; OR: outer ring.

Table 2. Performance metrics of different CRE configurations for *D*max/*Z* = 1. *D*max: maximum diameter; *Z*: dipole depth; Opt: optimal; NA: normalized amplitude; NME: normalized maximum error; NSS: normalized spatial selectivity.

Criteria	CRE		*D*max/*Z*	NA (%)	NME (%)	NSS (%)	NA/NME
Opt. (NME, NSS)	Bip1,3	)-)-----	1	2.7	3.0	96.4	0.90
Opt. (NA, NA/NME)	Bip1,9	)-------)	1	25.9	22.5	78.7	1.15
Opt. (NA)	Bip1-3,9	)))-----)	1	24.5	23.4	78.0	1.05
Makeyev *et al* 2022 [34]	Bip1,3-9	)-))))))	1	13.4	17.2	83.0	0.78
Spes Medica	Bip1-3,7-9	)))---)))	1	19.9	20.5	80.0	0.97
Opt. (NME, NSS, NA/NME)	Trip1,3,5	)-)-)----	1	2.7	0.2	99.5	12.10
Opt. (NA, NA/NME)	Trip1,7,9	)-----)-)	1	16.6	3.1	92.4	5.34
Opt. (NA)	Trip1-3,7,9	)))---)-)	1	15.3	3.4	91.7	4.50
Makeyev *et al* 2021 [29]	Trip1,3,5-9	)-)-))))))	1	2.7	0.6	98.6	4.75
CREmedical	Trip1-3,6,9	)))--)--)	1	11.0	2.6	93.6	4.23

maximizing the NA/NME would be those with the largest IAD and minimum pole widths, i.e. Bip1,9. For TCRE, the optimal candidates would be those with the largest IAD (CD-MR) and minimum pole widths, i.e. Trip1,7,9, and with the lowest IAD (CD-OR) and minimum pole widths, i.e. Trip1,3,5.

3.6. Optimal CRE selection methodology

One possible approach to choosing a CRE for a given application with specific approximate dipole depth and maximum electrode size would be to compare the performance metrics of different CREs looking for the most suitable configuration. Table 2 shows the values of the CRE performance metrics, in an example of application where *D*max/*Z* = 1, for the configurations that were proposed as optimal candidates with the previously presented criteria. Recently published optimal versions, minimizing the error of Laplacian estimation and with the outer diameter of the electrode equal to *D*max, as well as to the commercial BCREs from Spes Medica and TCREs from CREmedical, are also shown for additional comparison.

As can be observed from the table, the optimal candidate for BCREs in terms of the NME and NSS (Bip1,3) shows a small error (NME = 3%) and good SS (NSS = 96.4%), but its signal amplitude may be too small (NA = 2.7%). Conversely, the optimal candidates for BCREs in terms of the NA (Bip1,9; Bip1-3,9) show a 'large' signal amplitude (NA = 25.9%; 24.5%), but the error may not be acceptable (NME = 22.5%; 23.4%), along with a poor SS (NSS = 78.7%; 78.0%). Bip1,9 outperforms all other BCREs in terms of the balance between NA and NME. Similar arguments can be made about TCREs, although the NME in these cases is significantly smaller than

Table 3. Performance metrics and optimal *D*max/*Z* of different CRE configurations that fulfill NA $>$ 5%, NME $<$ 5% and NSS $>$ 95%. *D*max: maximum diameter; *Z*: dipole depth; Opt: optimal; NA: normalized amplitude; NME: normalized maximum error; NSS: normalized spatial selectivity.

Criteria	CRE		Optimal *D*max/*Z*	NA (%)	NME (%)	NSS (%)	NA/NME
Opt. (NA)	Bip1,9	)-------)	0.4	5.1	4.4	97.0	1.2
Opt. (NME, NSS)	Trip1,3,5	)-)-)----	1.4	5.1	0.8	99.0	6.6
Opt. (NA)	Trip1,7,9	)-----)-)	0.6	6.6	0.5	99.5	13.0
Opt. (NA)	Trip1-3,7,9	)))---)-)	0.6	6.1	0.6	99.5	11.0
Makeyev 2021	Trip1,3,5-9	)-)-))))))	1.4	5.1	1.8	97.5	2.9
CREmedical	Trip1-3,6,9	)))--)--)	0.7	5.8	0.7	99.8	7.8

Table 4. Physical dimensions of CRE shown in table 4 considering a dipole depth $Z = 14.3$ mm. CD: central disc; MR: middle ring; OR: outer ring.

CRE		CD (mm)	MR-inner (mm)	MR-outer (mm)	OR-inner (mm)	OR-outer (mm)
Bip1,9	)-------)	0.6	—	—	5.1	5.7
Trip1,3,5	)-)-)----	2.2	4.4	6.7	8.9	11.1
Trip1,7,9	)-----)-)	1.0	5.7	6.7	7.6	8.6
Trip1-3,7,9	)))---)-)	2.9	5.7	6.7	7.6	8.6
Trip1,3,5-9	)-)-)))))	2.2	4.4	6.6	8.9	20.0
CREmedical	)))--)--)	3.3	5.5	6.7	8.9	10.0

that of BCREs. Results for more CRE configurations could be listed and the final choice would depend on the prioritized performance metrics.

When using CREs to monitor the activity of a certain organ or muscle in order to avoid excessively weak signals, large Laplacian estimation error or poor SS, setting threshold levels for CRE metrics is recommended. By setting such thresholds, we can prioritize certain performance metrics while keeping others at acceptable levels. Each of these thresholds on performance metrics leads to a range of possible *D*max/*Z* values for each CRE configuration that meets the requested specifications.

An additional practical consideration should be made in this methodology for choosing/designing a CRE for a given application (given dipole depth, *Z*). This is linked to the discrete number of CRE configurations derived from using nine intervals in the finite dimensional model of the CREs, and it may be included in the discussion, but it is worth including it here and enriching the CRE selection methodology and associated results. The value of *D*max/*Z* for a given application could be considered an upper limit of that ratio rather than a constant value, since smaller values of *D*max could also be considered and hence more CRE designs with other absolute widths and IADs would be available to choose from.

This can be illustrated with an application example of $Z = 14$ mm and *D*max $= 2.5$ mm (upper limit of *D*max/*Z* $= 1.79$) and setting the threshold values to 0.05 (which is a typical threshold value in various contexts including but not limited to significance levels in statistical tests): NA $>$ 5%, NME $<$ 5% and NSS $>$ 95%. Setting the maximum value of NA/NME as additional criteria for the final choice of the *D*max/*Z* value for each configuration, the performance metrics and CRE dimensions of CRE designs from table 2 that fulfill the specifications are shown in tables 3 and 4, respectively.

All CRE configurations shown in table 3 meet the imposed thresholds but with remarkable differences in the value of NA/NME. The tripolar configurations clearly outperform the bipolar ones. Among the TCREs, Trip1,3,5-9 yields the lowest NA/NME (2.9) and Trip1,7,9 the highest (13.0), the latter being almost double that of the commercial version from CREmedical, which yields NA/NME $= 7.8$. It is also noteworthy that the greatest NA/NME is obtained for the lowest acceptable *D*max/*Z* in all the configurations, indicating a decrease in this parameter as *D*max/*Z* increases, as shown in figure 7.

Regarding the CRE dimensions, as can be seen in table 4, the dipole depth of the application example ($Z = 14.3$ mm) was chosen for the case where the dimensions of the optimal CREmedical configuration (Trip1-3,6,9) coincide with those of its commercial version. The optimal Bip1,9 configuration for this application would be of 5.7 mm in outer diameter, half of that of CREmedical, but also with worse performance metrics. Trip1,3,5-9 would be the largest electrode (20.0 mm) and with the worst performance metrics for TCREs. Trip1,3,5 would have a similar outer diameter of the electrode (11.1 mm) to that of CREmedical and slightly worse performance, as can be seen from table 3. Conversely, the results of this design process for Trip1,7,9 and Trip1-3,7,9 yield CREs of smaller outer diameters (8.6 mm). These electrodes showed enhanced performance metrics (larger NA and smaller NME in table 3) in comparison to Trip1,3,5 and CREmedical (Trip1-3,6,9) thanks to the enlarged IAD (CD-MR) and narrower ring widths.

4. Discussion

In this paper, we have carried out a comprehensive study of the influence of different aspects of the CRE design on their potential performance, by means of a finite dimensional model

of the electrode and finite element method modeling of the propagating volume of the bioelectrical activity.

4.1. Effect of dimensional parameters of CRE

Our results show that the larger the electrode the better in terms of the signal amplitude (and associated signal-to-noise ratio). This agrees with previous analytical and simulation results [29] as well as with experimental results from cardiac and uterine electromyographic signal recordings with a polymer BCRE, where larger electrodes, keeping the CD and pole widths constant, provided signals of larger amplitude and signal-to-noise ratio [22, 23]. Nonetheless, our results also show that larger electrodes entail larger Laplacian estimation errors and worse SS. Again, this agrees with the experimental results from cardiac signals, which were recorded with textile BCREs of two sizes [3]. Both electrodes had a CD radius of 16 mm and an outer ring width of 14 mm, while the outer diameter of the ring was changed from 42 mm to 50 mm. The amplitude of the different cardiac waves was about 35% larger for the larger electrode, while the SS was about 15%–25% smaller [3]. In the case of the Laplacian estimation error, since a reference to the 'true' Laplacian is needed, only analytical and simulation studies have been previously reported [24, 29, 30], which also show larger Laplacian estimation errors for larger electrodes.

Thanks to the use of a finite dimensional model of the electrode, where the dimensions of the CRE poles are not negligible, we have also observed that for the same outer diameter a larger signal amplitude can be obtained by increasing the inter-pole average distance by reducing the pole widths (as when we compared the NA of Bip1,9 for a given Dmax/Z with the NA of Bip1,3 for 3·Dmax/Z). Such a design keeps the Laplacian estimation error and SS almost constant. Thus, the first two conclusions can be derived: the pole widths of the electrodes should be as small as possible and a balance between the amplitude and Laplacian estimation error/SS should be considered when choosing the electrode size. Regarding the first conclusion, electrode designs such as the one in [21] with very narrow widths (CD diameter and pole widths of 0.4 mm, outer diameter 3.6 cm) are recommended. In contrast, the designs of BCRE from Spes Medica and TCRE in [35, 36], with pole widths equal to the gap between poles, could be optimized by narrowing their conductive recording surfaces. Designs with large CD and small inter-pole distances, such as those in [6] or those from CREmedical, could also be optimized according to our results. Nonetheless, this width reduction is mainly limited by two factors: the limits of the manufacturing technique and the impedance of the electrode poles. The first limit can largely vary depending on the technique, conductor material and electrode substrate, but may be on the order of tens of microns in a conservative scenario. Regarding the impedance of the pole (and that of the skin-to-electrode contact), it increases as its area diminishes. Nonetheless, current biosignal conditioning systems have very large input impedances [37] and can deal with large skin-to-electrode impedances.

With respect to the effects of the dimensional parameters of the CRE on the NME (and NSS), they generally showed opposite behaviors to the effects on the NA; i.e. what was favorable in terms of the NA was unfavorable in terms of the NME (and NSS). We computed the NA/NME ratio to study which effect is more acute and which CRE configuration reaches the best balance between maximizing the amplitude (and therefore the associated signal-to-noise ratio) and minimizing the error in the Laplacian estimation. For a given CRE configuration, greater values of this ratio are obtained for smaller electrodes; i.e. when increasing the electrode size, the desirable increase in amplitude is smaller than the undesirable increase in the error of the Laplacian estimation. The electrode should thus be as small as possible as long as the signal amplitude is large enough, which forms the third conclusion of this work. In this context, it should be considered that in TCREs the smallest bipolar signal amplitude is the one obtained from the differential voltage between the MR and the CD, and would thus be the most restrictive one in terms of the potential signal-to-noise ratio. Therefore, the signal quality would benefit from increasing the inter-pole distance between the MR and CD. In fact, as shown in tables 4 and 5, an electrode with such design (Trip1,7,9) yields a greater MR-CD signal amplitude than larger electrodes with the MR placed half way between the CD and the OR (Trip1,3,5 or commercial CREmedical electrodes) and even greater than designs with minimum distance between the CD and MR, as in Trip1,3,5-9 [29]. Furthermore, not only was the restrictive signal amplitude larger, the NME was also smaller. According to this, the fourth conclusion of this work is that the MR should be placed as far as possible from the CD; i.e. closer to the OR. Thus, we suggest modifying the usual configuration of the TCRE, where the distance between CD-MR equals that of MR-OR (constant inter-ring distance) as in the electrodes from CREmedical and [5, 27], and even more so those electrode designs where the MR is very close to CD while the OR is farther away (increasing the inter-ring distances), as in [12]. While it is true that, with the same outer electrode diameter, designs with increasing inter-ring distances yield the lowest Laplacian estimation errors, followed by constant and by decreasing inter-ring distances [25], they also yield a smaller signal amplitude and signal-to-noise ratio [38]. Similarly, previously reported optimal configurations of CRE [29], with the only criterion of minimizing the Laplacian estimation error and with the constraint that the outer diameter of the CRE should be Dmax, showed that the smallest NME of TCREs with the same 'true' outer diameter but also the smallest signal amplitude (table 2). Our results show that, without such constraints, when using a larger CD-MR distance and a smaller MR-OR distance, the resulting CRE can be of smaller outer dimensions, yielding an even smaller Laplacian estimation error and a larger MR-CD signal amplitude.

4.2. TCRE vs. BCRE

Another issue that should be discussed is the comparison between BCREs and TCREs. For the same outer diameter of the electrode, it is obvious that the amplitude of the bipolar signal from the BCRE would be greater than that of the bipolar signal obtained from the MR-CD of the TCRE, as confirmed

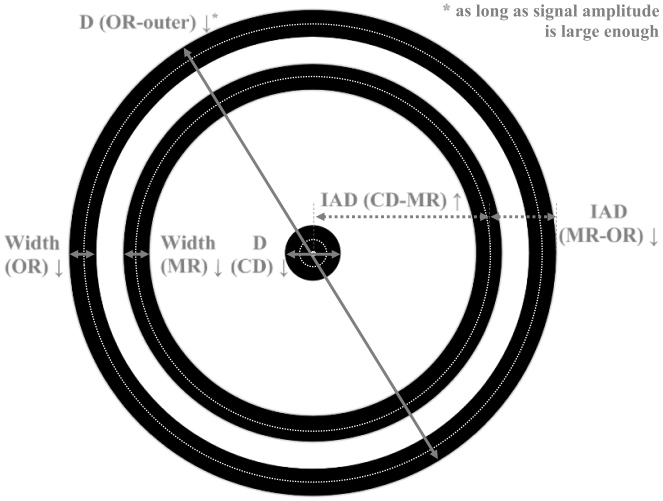

Figure 8. General criteria for dimensional parameters of optimal CRE. CD: central disc; MR: middle ring; OR: outer ring; D: diameter; IAD: inter-pole average distance.

with experimental results in [38]. Nonetheless, the NME that can be obtained with a BCRE is much larger than that of a TCRE of the same size (figure 4, also reported in [24, 30]), and still larger than a TCRE of double the size (tables 3 and 4). In fact, our results show that thresholding a maximum NME seriously limits the acceptable size of the BCRE for a given application. The SS is also worse for BCREs in comparison with TCREs (figure 5), which agrees with [5], which compared BCREs and TCREs in body surface electrocardiogram isochronal mapping. In that work, the tripolar configuration provided high spatial selectivity even for a larger electrode diameter (the TCRE was implemented by adding an OR while keeping the CD and MR of the BCRE). Our results suggest that a better balance between the signal amplitude and Laplacian estimation error (and SS) is obtained with TCREs. Therefore, another important conclusion of this work is that TCREs are highly recommended over BCREs. Even when the outer diameter of the electrode is restricted, it is worth adding another ring close to the OR so as not to significantly reduce the signal amplitude, to obtain higher Laplacian estimation accuracy and SS. Nonetheless, it should also be noted that to obtain the Laplacian estimate via TCRE, two bipolar signals (and associated additional signal instrumentation hardware) are needed, as opposed to only one needed for BCRE.

Figure 8 shows, in graphical form, the general criteria for the different dimensional parameters of the optimal CRE according to the considerations covered in this discussion.

4.3. Limitations of the study

This work is not exempt from limitations. The finite element method model used is simple; it does not consider body curvature and is single-layer. The results would be more realistic with a more comprehensive model, such as a five-layer planar model of the abdomen [39] or the four-layer concentric inhomogeneous spherical head model used in [6]. Including layers with different conductivities and thicknesses or considering multi-dipole sources rather than a single one will undoubtedly significantly change the characteristics of signals on the body surface, but the conclusions derived from the comparison of different configurations of CREs will remain similar — even more so, considering that all the performance metrics are normalized in this study. Furthermore, the comparison with experimental data (when available), discussed above, supports our results. Another potential limitation is the NA and NME being considered of equal importance in the utilized NA/NME ratio. Depending on the application, this can change from the NME being of greater importance in the case of a high signal-to-noise ratio, to the NA being of greater importance in the case of a low signal-to-noise ratio. However, this limitation can be addressed for a specific application by modifying either the threshold values for NA and NME in the proposed methodology or the NA/NME ratio accordingly. For example, for an application with high signal-to-noise ratio, NA/NME^2 can be used instead.

5. Conclusions

In this work we carried out a comprehensive comparison of BCREs and TCREs, specifically assessing, for the first time, the influence of design issues such as the maximum electrode size, pole widths and inter-pole distances on their performance in terms of the signal amplitude (and therefore quality), Laplacian estimation error and SS.

The main conclusions derived from our analysis and results are: (1) the CRE should be as small as possible, as long as the signal amplitude is large enough; (2) the pole widths should be as small as possible; (3) the middle ring of the TCRE should be as far as possible from the CD; (4) TCREs typically outperform BCREs of the same outer electrode diameter, significantly reducing the Laplacian estimation error and improving the SS at the cost of a small decrease in signal amplitude; (5) the design of current commercial versions of CRE could be optimized.

Furthermore, the methodology presented in this work permits comparison of the expected performance of different CRE configurations for a given application, taking into consideration practical aspects such as the depth of activity sources and/or the maximum size of electrodes to be used. In this way, CRE configurations can be selected based on the specification set for CRE performance.

The monitoring and analysis of bioelectrical signals in a wide range of applications where CREs have shown their advantage in comparison with conventional disc electrodes, such as electrocardiography, electroencephalography and electromyography of uterine, swallowing, gastrointestinal or breathing muscles, can benefit from the enhanced electrode designs and methodology proposed in this work.

Data availability statement

The data cannot be made publicly available upon publication because they are not available in a format that is sufficiently

accessible or reusable by other researchers. The data that support the findings of this study are available upon reasonable request from the authors.

Funding

This research was funded by the National Science Foundation (NSF) Division of Human Resource Development (HRD) Tribal Colleges and Universities Program (TCUP), Grant Number 2212707, to O M.

Author contributions

Conceptualization, O M and J G-C; methodology, O M, Y Y-L, G P-B and J G-C; software, O M and Y Y-L; validation, O M, Y Y-L, G P-B and J G-C; formal analysis, O M and Y Y-L; writing—original draft preparation J G-C; writing—review and editing, O M, Y Y-L, G P-B and J G-C; visualization, Y Y-L; supervision, J G-C; funding acquisition, O M. All authors have read and agreed to the published version of the manuscript.

Conflict of interest

The authors declare no conflict of interest. The funders had no role in the design of the study; in the collection, analyses or interpretation of data; in the writing of the manuscript; or in the decision to publish the results.

ORCID iDs

Javier Garcia-Casado https://orcid.org/0000-0003-1410-2721
Yiyao Ye-Lin https://orcid.org/0000-0003-2929-181X
Gema Prats-Boluda https://orcid.org/0000-0002-9362-5055
Oleksandr Makeyev https://orcid.org/0000-0003-2648-0500

References

[1] Besio W G, Koka K, Aakula R and Dai W 2006 Tri-polar concentric ring electrode development for laplacian electroencephalography *IEEE Trans. Biomed. Eng.* **53** 926–33
[2] He B and Cohen R J 1992 Body surface Laplacian ECG mapping *IEEE Trans. Biomed. Eng.* **39** 1179–91
[3] Prats-Boluda G, Ye-Lin Y, Pradas-Novella F, Garcia-Breijo E and Garcia-Casado J 2018 Textile concentric ring electrodes: influence of position and electrode size on cardiac activity monitoring *J. Sens.* **2018** 1–9
[4] Prats-Boluda G, Guillem M S, Rodrigo M, Ye-Lin Y and Garcia-Casado J 2022 Identification of atrial fibrillation drivers by means of concentric ring electrodes *Comput. Biol. Med.* **148** 105957
[5] Besio W and Chen T 2007 Tripolar Laplacian electrocardiogram and moment of activation isochronal mapping *Physiol. Meas.* **28** 515–29
[6] Liu X, Makeyev O and Besio W 2020 Improved spatial resolution of electroencephalogram using tripolar concentric ring electrode sensors *J. Sens.* **2020** 1–9
[7] Toole C, Martinez-Juárez I E, Gaitanis J N, Blum A, Sunderam S, Ding L, DiCecco J and Besio W G 2019 Source localization of high-frequency activity in tripolar electroencephalography of patients with epilepsy *Epilepsy Behav.* **101** 106519
[8] Estrada-Petrocelli L, Torres A, Sarlabous L, Rafols-de-urquia M, Ye-Lin Y, Prats-Boluda G, Jane R and Garcia-Casado J 2021 Evaluation of respiratory muscle activity by means of concentric ring electrodes *IEEE Trans. Biomed. Eng.* **68** 1005–14
[9] Alberola-Rubio J, Prats-Boluda G, Ye-Lin Y, Valero J, Perales A and Garcia-Casado J 2013 Comparison of non-invasive electrohysterographic recording techniques for monitoring uterine dynamics *Med. Eng. Phys.* **35** 1736–43
[10] Zena-Giménez V, Garcia-Casado J, Ye-Lin Y, Garcia-Breijo E and Prats-Boluda G 2018 A flexible multiring concentric electrode for non-invasive identification of intestinal slow waves *Sensors* **18** 396
[11] Ye-Lin Y, Martinez-De-Juan J L, Jareño-Silvestre A and Prats-Boluda G 2022 Concentric ring electrodes for non-invasive recording of gastric myoelectric activity *J. Int. Meas. Confed.* **188** 110607
[12] Wang K, Parekh U, Pailla T, Garudadri H, Gilja V and Ng T N 2017 Stretchable dry electrodes with concentric ring geometry for enhancing spatial resolution in electrophysiology *Adv. Healthcare Mater.* **6** 1700552
[13] Hiyama T, Sakurazawa S, Toda M, Akita J, Kondo K and Nakamura Y 2014 Motion estimation of five fingers using small concentric ring electrodes for measuring surface electromyography *2014 IEEE 3rd Global Conf. on Consumer Electronics (GCCE)* pp 376–80
[14] Castroflorio T, Deregibus A, Bargellini A, Debernardi C and Manfredini D 2014 Detection of sleep bruxism: comparison between an electromyographic and electrocardiographic portable holter and polysomnography *J. Oral Rehabil.* **41** 163–9
[15] Garcia-Casado J, Prats-Boluda G, Ye-Lin Y, Restrepo-Agudelo S, Perez-Giraldo E and Orozco-Duque A 2020 Evaluation of swallowing related muscle activity by means of concentric ring electrodes *Sensors* **20** 1–15
[16] Farina D and Cescon C 2001 Concentric-ring electrode systems for noninvasive detection of single motor unit activity *IEEE Trans. Biomed. Eng.* **48** 1326–34
[17] Estrada L, Torres A, Garcia-Casado J, Prats-Boluda G and Jane R 2013 Characterization of Laplacian surface electromyographic signals during isometric contraction in biceps brachii *2013 35th Annual Int. Conf. IEEE Engineering in Medicine and Biology Society (EMBC)* vol 2013 pp 535–8
[18] Besio W G *et al* 2014 High-frequency oscillations recorded on the scalp of patients with epilepsy using tripolar concentric ring electrodes *IEEE J. Transl. Eng. Health Med.* **2** 2000111
[19] Kaufer M, Rasquinha L and Tarjan P 1990 Optimization Of multi-ring sensing electrode set *Proc. of the Twelfth Annual Int. Conf. of the IEEE Engineering in Medicine and Biology Society* (*Philadelphia, PA, USA*) pp 612–3
[20] Prats-Boluda G, Ye-Lin Y, Bueno Barrachina J M, Senent E, De Sanabria R R and Garcia-Casado J 2015 Development of a portable wireless system for bipolar concentric ECG recording *Meas. Sci. Technol.* **26** 075102
[21] Besio W, Aakula R, Koka K and Dai W 2006 Development of a tri-polar concentric ring electrode for acquiring accurate Laplacian body surface potentials *Ann. Biomed. Eng.* **34** 426–35

[22] Ye-Lin Y, Alberola-Rubio J, Prats-boluda G, Perales A, Desantes D and Garcia-Casado J 2015 Feasibility and analysis of bipolar concentric recording of electrohysterogram with flexible active electrode *Ann. Biomed. Eng.* **43** 968–76

[23] Ye-Lin Y, Bueno-Barrachina J M, Prats-boluda G, Rodriguez de Sanabria R and Garcia-Casado J 2017 Wireless sensor node for non-invasive high precision electrocardiographic signal acquisition based on a multi-ring electrode *J. Int. Meas. Confed.* **97** 195–202

[24] Makeyev O, Ding Q and Besio W G 2016 Improving the accuracy of Laplacian estimation with novel multipolar concentric ring electrodes *Measurement* **80** 44–52

[25] Makeyev O and Besio W 2016 Improving the accuracy of Laplacian estimation with novel variable inter-ring distances concentric ring electrodes *Sensors* **16** 858

[26] Makeyev O, Lee C and Besio W G 2017 Proof of concept Laplacian estimate derived for noninvasive tripolar concentric ring electrode with incorporated radius of the central disc and the widths of the concentric rings *2017 39th Annual Int. Conf. IEEE Engineering in Medicine and Biology Society (EMBC)* vol 2017 pp 841–4

[27] Makeyev O, Musngi M, Moore L, Ye-Lin Y, Prats-Boluda G and Garcia-Casado J 2019 Validating the comparison framework for the finite dimensions model of concentric ring electrodes using human electrocardiogram data *Appl. Sci.* **9** 4279

[28] Makeyev O 2020 Comprehensive optimization of the tripolar concentric ring electrode with respect to the accuracy of Laplacian estimation based on the finite dimensions model of the electrode *Eng. Proc.* **2** 56

[29] Makeyev O, Ye-Lin Y, Prats-Boluda G and Garcia-Casado J 2021 Comprehensive optimization of the tripolar concentric ring electrode based on its finite dimensions model and confirmed by finite element method modeling *Sensors* **21** 5881

[30] Makeyev O 2018 Solving the general inter-ring distances optimization problem for concentric ring electrodes to improve Laplacian estimation *Biomed. Eng. Online* **17** 117

[31] He B and Wu D 1999 Laplacian electrocardiography *Crit. Rev. Biomed. Eng.* **27** 285–338 (available at: www.scopus.com/record/display.uri?eid=2-s2.0-0033501046&origin=inward&txGid=3bd50e19fce0efcf134e5f5dd85bcc8d)

[32] Besio W G and Fasiuddin M 2005 Quantizing the depth of bioelectrical sources for non-invasive 3D imaging *J. Bioelectromagn.* **7** 90–93

[33] Mei Z, Zhao N, Yang B and Liu J 2021 Flexible concentric ring electrode array for low-noise and non-invasive detection *Proc. IEEE Int. Conf. on Micro Electro Mechanical Systems* vol 2021 pp 266–9

[34] Makeyev O, Ye-Lin Y, Prats-Boluda G and Garcia-Casado J 2022 Comparing optimal and commercially available bipolar and tripolar concentric ring electrode configurations using finite element method modeling based on their finite dimensions models *IEEE Sensors Applications Symp. (SAS)* pp 1–5

[35] Liu X, Makeyev O and Besio W 2011 A comparison of tripolar concentric ring electrode and spline Laplacians on a four-layer concentric spherical model (https://doi.org/10.0/Linux-x86_64)

[36] Besio W G, Hongbao Cao H and Peng Zhou P 2008 Application of tripolar concentric electrodes and prefeature selection algorithm for brain–computer interface *IEEE Trans. Neural Syst. Rehabil. Eng.* **16** 191–4

[37] Song S, Zhou Y, Li M and Zhao M 2021 A review on recent development of input impedance boosting for bio-potential amplifiers *Proc.—Int. SoC Des. Conf. 2021, ISOCC 2021* pp 272–3

[38] Garcia-Casado J, Ye-Lin Y, Prats-Boluda G and Makeyev O 2019 Evaluation of bipolar, tripolar, and quadripolar Laplacian estimates of electrocardiogram via concentric ring electrodes *Sensors* **19** 3780

[39] Garcia-Casado J, Zena V, Perez J J, Prats-Boluda G, Ye-Lin Y and Garcia-Breijo E 2014 Opened-ring electrode array for enhanced non-invasive monitoring of bioelectrical signals: application to surface EEnG recording BIOSTEC 2013: *Biomedical Engineering Systems and Technologies* (*Communications in Computer and Information Science* vol 452) ed M Fernández-Chimeno *et al* (Springer) (https://doi.org/10.1007/978-3-662-44485-6_3)